



HAL
open science

Beam focusing by near-field transition radiation

S Corde, M Gilljohann, X Davoine, L Gremillet, A Sampath, M Tamburini

► **To cite this version:**

S Corde, M Gilljohann, X Davoine, L Gremillet, A Sampath, et al.. Beam focusing by near-field transition radiation. [Research Report] IP Paris; CEA; MPIK. 2020. hal-02937777v1

HAL Id: hal-02937777

<https://polytechnique.hal.science/hal-02937777v1>

Submitted on 14 Sep 2020 (v1), last revised 24 Feb 2021 (v2)

HAL is a multi-disciplinary open access archive for the deposit and dissemination of scientific research documents, whether they are published or not. The documents may come from teaching and research institutions in France or abroad, or from public or private research centers.

L'archive ouverte pluridisciplinaire **HAL**, est destinée au dépôt et à la diffusion de documents scientifiques de niveau recherche, publiés ou non, émanant des établissements d'enseignement et de recherche français ou étrangers, des laboratoires publics ou privés.

Beam focusing by near-field transition radiation

S. Corde¹, M. Gilljohann¹, X. Davoine², L. Gremillet², A. Sampath³,
and M. Tamburini³

¹IP Paris, France

²CEA, France

³MPIK, Germany

Contents

| | | |
|----------|-------------------------------------------------------------|----------|
| 1 | Introduction | 1 |
| 2 | Analytical estimates | 1 |
| 2.1 | Effective focal length for the beam central slice | 1 |
| 2.2 | Beam evolution with a single foil | 2 |
| 2.3 | Effect of multiple scattering | 4 |

1 Introduction

The goal of this document is to assess the possibility to measure and demonstrate a beam focusing effect from near-field coherent transition radiation (NF-CTR) using beam parameters that can be realistically achieved by the FACET-II facility at SLAC.

2 Analytical estimates

2.1 Effective focal length for the beam central slice

In SI units, the self-fields of an ultrarelativistic Gaussian particle beam are essentially transverse, and can be approximated as:

$$E_r^b(r, z, t) = \frac{qN}{(2\pi)^{3/2}\sigma_{\parallel}\epsilon_0 r} \left(1 - e^{-r^2/(2\sigma_{\perp}^2)}\right) e^{-\frac{(z-vt)^2}{2\sigma_{\parallel}^2}} \quad (1)$$

$$B_{\theta}^b(r, z, t) = \frac{qN}{(2\pi)^{3/2}\sigma_{\parallel}c\epsilon_0 r} \left(1 - e^{-r^2/(2\sigma_{\perp}^2)}\right) e^{-\frac{(z-vt)^2}{2\sigma_{\parallel}^2}}, \quad (2)$$

with $q = -e$ for an electron beam. The beam is taken to be centered at $\xi \equiv z - ct = 0$. We assume that the self-fields are perfectly reflected by the conductor, which is

reasonable if $\sigma_{\perp} \gtrsim \sigma_{\parallel}$. If the conductor's boundary is located at $z = 0$, the NF-CTR fields can therefore be written as:

$$E_r^c(r, z, t) = -\frac{qN}{(2\pi)^{3/2}\sigma_{\parallel}\epsilon_0 r} \left(1 - e^{-r^2/(2\sigma_{\perp}^2)}\right) e^{-\frac{(z+vt)^2}{2\sigma_{\parallel}^2}} \quad (3)$$

$$B_{\theta}^c(r, z, t) = \frac{qN}{(2\pi)^{3/2}\sigma_{\parallel}c\epsilon_0 r} \left(1 - e^{-r^2/(2\sigma_{\perp}^2)}\right) e^{-\frac{(z+vt)^2}{2\sigma_{\parallel}^2}}, \quad (4)$$

where the superscript c expresses that these fields are induced by the conductor. The above expressions obviously satisfy the boundary conditions at the conductor's surface: $E_r^c(r, 0, t) = -E_r^b(r, 0, t)$ and $B_{\theta}^c(r, 0, t) = B_{\theta}^b(r, 0, t)$.

We are now interested in the beam evolution in the (x, p_x) phase space. An electron in the central slice of the beam ($z = vt$), and with $x > 0$ and $y = 0$ ($r = x$), thus experiences a transverse momentum kick before hitting the conductor:

$$\begin{aligned} \Delta p_x &= \int_{-\infty}^0 q(E_x^c - vB_y^c) dt \simeq -2qc \int_{-\infty}^0 B_{\theta}^c(r = x, z = vt, t) dt \\ &= -\frac{2q^2 N}{(2\pi)^{3/2}\epsilon_0\sigma_{\parallel}x} \left(1 - e^{-x^2/2(\sigma_{\perp}^2)}\right) \int_{-\infty}^0 e^{-2(vt/\sigma_{\parallel})^2} dt \\ &\simeq -\frac{q^2 N}{4\pi\epsilon_0 cx} \left(1 - e^{-x^2/2(\sigma_{\perp}^2)}\right) \\ &\simeq -\frac{q^2 Nx}{8\pi\epsilon_0 c\sigma_{\perp}^2}, \end{aligned} \quad (5)$$

where the last approximation holds for $x \lesssim \sigma_{\perp}$. From Eq. (5), the angular kick is $\Delta\theta_x \simeq \Delta p_x/p_z \simeq \Delta p_x/(\gamma mc) = -q^2 Nx/(8\pi\epsilon_0\sigma_{\perp}^2\mathcal{E})$, where $\mathcal{E} = \gamma mc^2$ is the particle energy. For a perfect thin lens of focal length f , the angular kick writes $\Delta\theta_x = -x/f$. We thus deduce the effective focal length for the beam central slice of the near-field transition radiation focusing effect:

$$f = \frac{8\pi\epsilon_0\sigma_{\perp}^2\mathcal{E}}{q^2 N} \quad (6)$$

In physical units and for $|q| = e$, this writes:

$$f[\text{mm}] = 0.2225 \frac{\sigma_{\perp}[\mu\text{m}]^2 \mathcal{E}[\text{GeV}]}{Q[\text{nC}]} \quad (7)$$

Note that the result is independent of the bunch length, because the self fields are inversely proportional to σ_{\parallel} but the focusing effect is integrated over the bunch length. However, by using perfect reflected fields we have assumed $\sigma_{\parallel} \lesssim \sigma_{\perp}$, and therefore the bunch length cannot be arbitrarily chosen; it needs to be smaller than the beam size for the desired focal length. Table 1 shows a few examples of focal length values for different beam sizes.

2.2 Beam evolution with a single foil

To understand if this foil focusing effect will be measurable, we need to account for the finite beam emittance and the multiple scattering in the foil.

| Beam size | Focal length |
|--------------------|-------------------|
| 30 μm | 1.0 m |
| 10 μm | 110 mm |
| 3 μm | 10 mm |
| 1 μm | 1.1 mm |
| 0.55 μm | 340 μm |

Table 1: Examples of focal length values for different beam sizes and for $Q = 2$ nC and $\mathcal{E} = 10$ GeV. 0.55 μm is the beam size value used in [A. Sampath *et al.*, arXiv:2009.01808 \[physics.plasma-ph\] \(2020\)](#).

The transport matrix associated to the NF-CTR-induced lens is:

$$M = \begin{pmatrix} 1 & 0 \\ -1/f & 1 \end{pmatrix} \quad (8)$$

and the beam Twiss parameters after experiencing NF-CTR are:

$$\alpha_2 = -M_{11}M_{21}\beta_1 + (M_{11}M_{22} + M_{12}M_{21})\alpha_1 - M_{12}M_{22}\gamma_1 \quad (9)$$

$$\beta_2 = M_{11}^2\beta_1 - 2M_{11}M_{12}\alpha_1 + M_{12}^2\gamma_1 \quad (10)$$

and they simplify to:

$$\alpha_2 = \alpha_1 + \beta_1/f \quad (11)$$

$$\beta_2 = \beta_1 \quad (12)$$

where $(\alpha_1, \beta_1, \gamma_1)$ and $(\alpha_2, \beta_2, \gamma_2)$ are the beam Twiss parameters respectively just before and just after experiencing NF-CTR, and $\gamma_{1,2} = (1 + \alpha_{1,2}^2)/\beta_{1,2}$.

If the waist is initially at the foil ($\alpha_1 = 0$), then the new waist after the beam has experienced NF-CTR is:

$$s^* = \alpha_2\beta_2^* = \frac{\alpha_2\beta_2}{1 + \alpha_2^2} \quad (13)$$

$$= f \frac{\beta^2}{\beta^2 + f^2} \quad (14)$$

where $\beta = \beta_2 = \beta_1$. To have a waist shift similar to the focal length ($s^* \sim f$), one needs $f \ll \beta$.

A second important parameter is the beam divergence. If the beam divergence changes substantially due to NF-CTR, this gives us a way to measure and demonstrate the NF-CTR effect in the experiment. The beam divergence before and after NF-CTR read:

$$\theta_1 = \sqrt{\epsilon_g(1 + \alpha_1^2)/\beta_1} \quad (15)$$

$$\theta_2 = \sqrt{\epsilon_g(1 + \alpha_2^2)/\beta_2} \quad (16)$$

where ϵ_g is the beam geometrical emittance. Again, if the waist is initially at the foil ($\alpha_1 = 0$), then we have:

$$\theta_2 = \theta_1 \sqrt{1 + (\beta/f)^2} \quad (17)$$

| Normalized emittance | β/f |
|----------------------|-----------|
| $100 \mu\text{m}$ | 0.176 |
| $30 \mu\text{m}$ | 0.586 |
| $10 \mu\text{m}$ | 1.76 |
| $3 \mu\text{m}$ | 5.86 |

Table 2: Examples of values of the figure of merit β/f for different normalized emittances and for $Q = 2 \text{ nC}$.

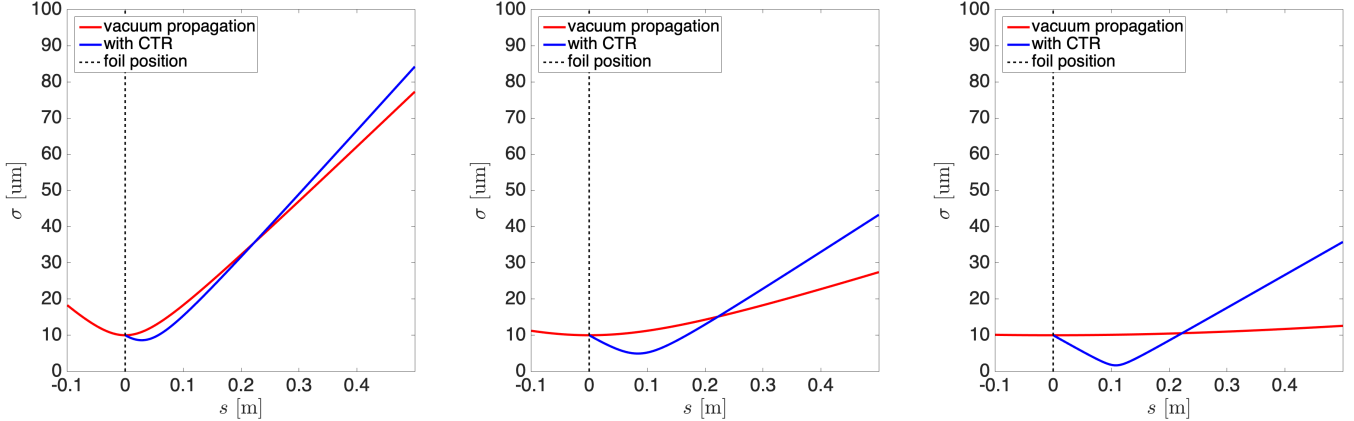


Figure 1: **Beam evolution and focusing effect from near-field transition radiation.** Evolution of the beam size with the propagation distance with and without foil, for normalized emittances of $30 \mu\text{m}$ (left), $10 \mu\text{m}$ (middle) and $3 \mu\text{m}$ (right), and for an initial waist located at the foil position and for a beam size of $10 \mu\text{m}$ at the waist. The effect of multiple scattering is not taken into account.

Similarly to the waist shift, we see that the effect is strong and measurable for $f \ll \beta$.

A good figure of merit to determine whether NF-CTR focusing is measurable is therefore the ratio β/f (for $\beta/f \gtrsim 1$, the effect can easily be demonstrated experimentally). We have:

$$\beta/f = \frac{q^2 N}{8\pi\epsilon_0 m c^2 \epsilon_n} = 8.794 \frac{Q[\text{nC}]}{\epsilon_n[\mu\text{m}]} \quad (18)$$

with $\epsilon_n = \gamma\epsilon_g$ the normalized emittance of the beam. Interestingly, we see that this figure of merit does not depend on the beam size, but only depends on the charge and normalized emittance. Table 2 shows a few examples of values for this figure of merit β/f for different normalized emittances.

Figure 1 shows the evolution of the beam size during propagation with and without the foil, for different normalized emittances. The result shows that for an emittance of $30 \mu\text{m}$, the NF-CTR focusing effect is measurable, but to use it to reach significantly smaller beam size at the new waist, an emittance of $3 \mu\text{m}$ is much more promising.

2.3 Effect of multiple scattering

Multiple scattering in the foil can be detrimental in increasing the angular spread and emittance of the beam, and in preventing its focusing to very small spot size at

the new waist. The rms scattering angle due to multiple scattering in the foil writes (see The Review of Particle Physics (2020), P.A. Zyla et al. (Particle Data Group), Prog. Theor. Exp. Phys. 2020, 083C01 (2020), section 34.3 Multiple scattering through small angles):

$$\theta_s = \frac{13.6}{\mathcal{E}[\text{MeV}]} \sqrt{d/X_0} [1 + 0.038 \ln(d/X_0)] \quad (19)$$

where X_0 is the radiation length of the material and d its thickness. For aluminum, $X_0 = 8.897$ cm. Table 3 shows a few examples of scattering angle values for an aluminum foil and for different thicknesses.

To assess the importance of this multiple scattering effect, the scattering angle should be compared to $\sqrt{\epsilon_g/\beta}$, where $\beta = \beta_2 = \beta_1$ is the beta function before multiple scattering. If the waist is located at the foil, $\alpha_1 = 0$ and $\sqrt{\epsilon_g/\beta}$ corresponds to the beam divergence θ_1 , before the beam has experienced NF-CTR.

For a beam size of $10 \mu\text{m}$ and a normalized emittance of $30 \mu\text{m}$, $\theta_1 = 153 \mu\text{rad}$. In this case, even for a $100\text{-}\mu\text{m}$ -thick Al foil, multiple scattering will not compromise our ability to demonstrate NF-CTR focusing, the increase in beam divergence is still dominated by NF-CTR, see Fig. 2 and Table 4.

For a beam size of $10 \mu\text{m}$ and a normalized emittance of $3 \mu\text{m}$, $\theta_1 = 15.3 \mu\text{rad}$. In this case, a $100\text{-}\mu\text{m}$ -thick Al foil will significantly limit our capability to focus the beam to very small spot sizes using NF-CTR. A micrometer-thick Al foil is thus desired in this case. Indeed, in Fig. 3, we see that for an Al thickness of $100 \mu\text{m}$, multiple scattering considerably increases the spot size at the new waist, by more than a factor of 2. For an Al thickness of $10 \mu\text{m}$, a weak effect is still visible, while for $1 \mu\text{m}$ thickness the curves with or without multiple scattering overlap.

| Al thickness | Scattering angle (rms) |
|-------------------|------------------------|
| $100 \mu\text{m}$ | $34 \mu\text{rad}$ |
| $10 \mu\text{m}$ | $9.4 \mu\text{rad}$ |
| $1 \mu\text{m}$ | $2.6 \mu\text{rad}$ |
| $0.5 \mu\text{m}$ | $1.7 \mu\text{rad}$ |

Table 3: Examples of scattering angle values for $\mathcal{E} = 10$ GeV and for an aluminum foil of different thicknesses. $0.5 \mu\text{m}$ is the Al thickness used in A. Sampath et al., arXiv:2009.01808 [physics.plasma-ph] (2020).

| Conditions | Beam divergence (rms) |
|------------------------------|-----------------------|
| No foil | $153 \mu\text{rad}$ |
| NF-CTR only | $178 \mu\text{rad}$ |
| Multiple scattering only | $157 \mu\text{rad}$ |
| NF-CTR + multiple scattering | $181 \mu\text{rad}$ |

Table 4: Beam divergence for different conditions. Here the beam parameters are the same as for Fig. 2: the normalized emittance is $30 \mu\text{m}$, the beam size is $10 \mu\text{m}$, the charge is 2 nC, the beam energy is 10 GeV, and the Al foil has a thickness of $100 \mu\text{m}$.

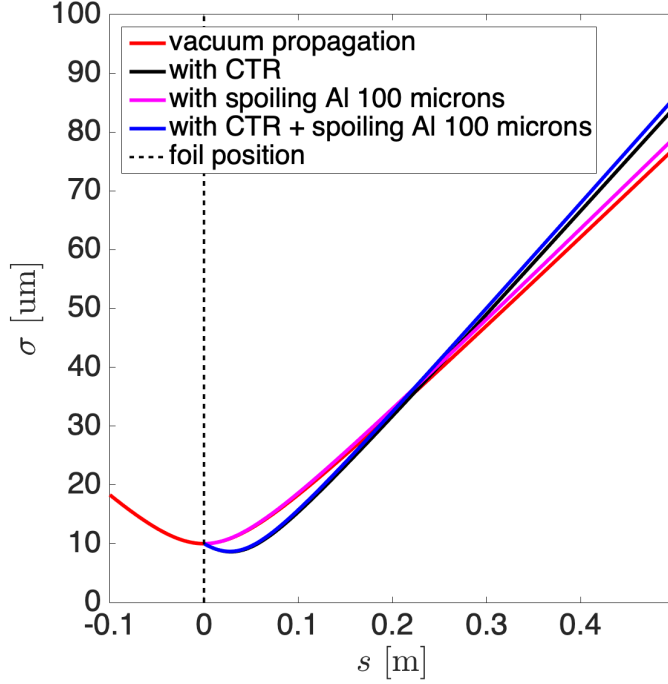


Figure 2: **Beam evolution with multiple scattering included and $30 \mu\text{m}$ normalized emittance.** Evolution of the beam size with the propagation distance with and without foil, for an initial waist located at the foil position and for a beam size of $10 \mu\text{m}$ at the waist. The effect of multiple scattering is taken into account for an aluminum foil of $100 \mu\text{m}$ thickness.

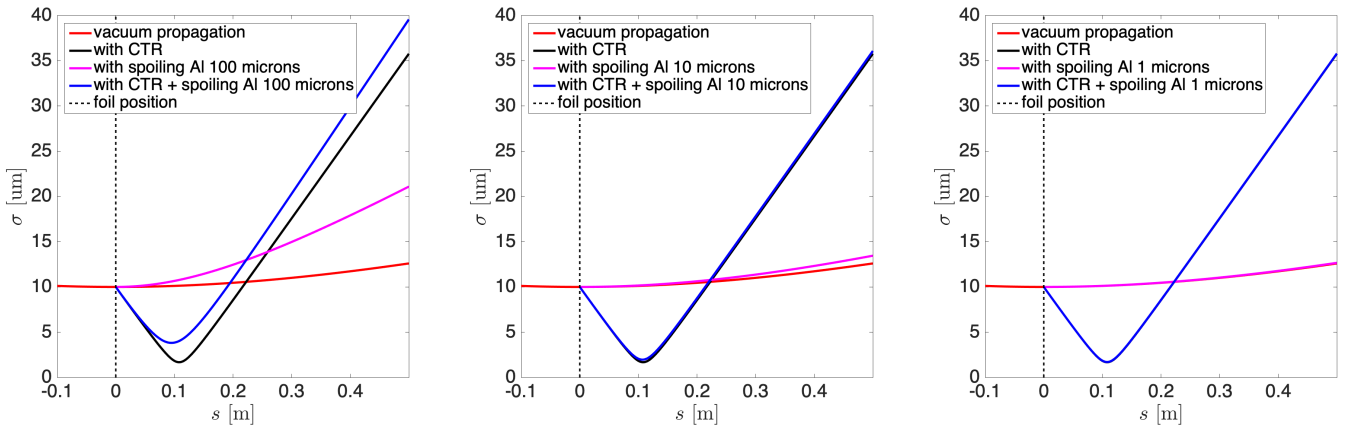


Figure 3: **Beam evolution with multiple scattering included and $3 \mu\text{m}$ normalized emittance.** Evolution of the beam size with the propagation distance with and without foil, for an initial waist located at the foil position and for a beam size of $10 \mu\text{m}$ at the waist. The effect of multiple scattering is taken into account for an aluminum foil with a thickness of $100 \mu\text{m}$ (left), $10 \mu\text{m}$ (middle) and $1 \mu\text{m}$ (right).